Eek RA, Dijkstra SJ and van Rosmalen GM (1995b) Dynamic modelling of suspension crystallizers, using experimental data. *American Institute of Chemical Engineers Journal* 41(3): 571–584.

Kramer HJM, Bermingham SK and van Rosmalen GM (1999) Design of industrial crystallisers for a required product quality. *Journal of Crystal Growth* 198/199: 729–737.

Miller SM and Rawlings JB (1994) Model identification and control strategies for catch cooling crystallisers. *American Institute of Chemical Engineers Journal* 40: 1312–1327.

Ó Meadhra RS, Kramer HJM and van Rosmalen GM (1995) A model for secondary nucleation in a suspension crystallizer. *American Institute of Chemical Engineers Journal* 42(4): 973–982.

Randolph AD and Larson MA (1988) *Theory of Particulate Processes*, 2nd edn. New York, Academic Press.

Randolph AD, Chen L and Tavana A (1987) A feedback control of CSD in a KCl crystallisation with fines dissolver. *American Institute of Chemical Engineers Journal* 33: 582–591.

Randolph AD, Beckman JR and Kralievich ZI (1977) Crystal size distribution dynamics in a classified crystalliser: part 1, experimental and theoretical study of cycling in a potassium chloride crystallisation. *American Institute of Chemical Engineers Journal* 23: 500–510.

Rawlings JB, Miller SM and Witkowski WR (1993) Model identification and control of solution crystallisation processes. *Industrial and Engineering Chemistry Research* 32: 1275–1296.

Rawlings JB, Sink CW and Miller SM (1995) Control of crystallisation processes. In: Meyerson A (ed.) *Handbook of Industrial Crystallisation*, pp. 103–130. Boston: Butterworth Heinemann.

Redman T, Rohani S and Strathdee G (1997) Control of the crystal mean size in a pilot plant potash crystalliser. *Transactions of the Institute of Chemical Engineers* 75A: 183–192.

Rohani S (1995) Control of crystallisers. In: Mersmann A (ed.), *Crystallisation Technology Handbook*. New York: Marcel Dekker, Inc.

Dynamic Behaviour

See **II / CRYSTALLIZATION / Control of Crystallizers and Dynamic Behaviour**

DropBooks

Geocrystallization

J. A. Gamble, School of Earth Sciences, Victoria University of Wellington, New Zealand

Copyright © 2000 Academic Press

Magmas are hot (eruption temperatures range between 600°C and 1400°C), multicomponent, but generally silicate-dominated melt systems formed by processes of partial melting in the interior of the earth. Silicon and oxygen are the major constituents of most magmatic systems, apart from those of the carbonatite association, where $NaCO_3$ and $CaCO_3$ are significant components. This article considers crystallization in silicate-dominated melt systems. In addition to Si and O, Ti, Al, Fe^{3+}, Fe^{2+}, Mn, Mg, Ca, Na, K and P comprise the constituents commonly referred to as the 'major elements'. It has become conventional to refer to these in terms of their oxides, expressed in weight percent (**Table 1**). Furthermore, magmas typically contain dissolved volatile species, dominated by H_2O, but including SO_2, H_2S, Cl_2, F_2, CO_2, CO and traces of noble gases such as He, Ar and Xe. Elements such as Rb, Sr, Ba, Zr, Nb, the rare earth elements, Pb, Th and U are present in trace amounts (typically μg g^{-1} or ppm) and are called 'trace elements'.

After magmas form, they may move away and separate from their source regions, due principally to

Table 1 Major oxide chemical analyses (wt%) of typical volcanic igneous rocks. All data are from the author's database of chemical analyses

Element oxide	*Basalt*	*Andesite*	*Dacite*	*Rhyolite*
SiO_2	49.86	60.35	66.68	73.89
TiO_2	1.38	0.78	0.58	0.33
Al_2O_3	15.96	17.53	16.5	13.69
Fe_2O_3	5.47	3.37	2.42	1.47
FeO	6.47	3.17	1.93	0.89
MnO	0.32	0.18	0.06	0.08
MgO	6.27	2.79	1.43	0.39
CaO	9.1	5.87	3.51	1.22
Na_2O	3.16	3.63	4.03	3.43
K_2O	1.55	2.07	2.71	4.53
P_2O_5	0.46	0.26	0.15	0.08

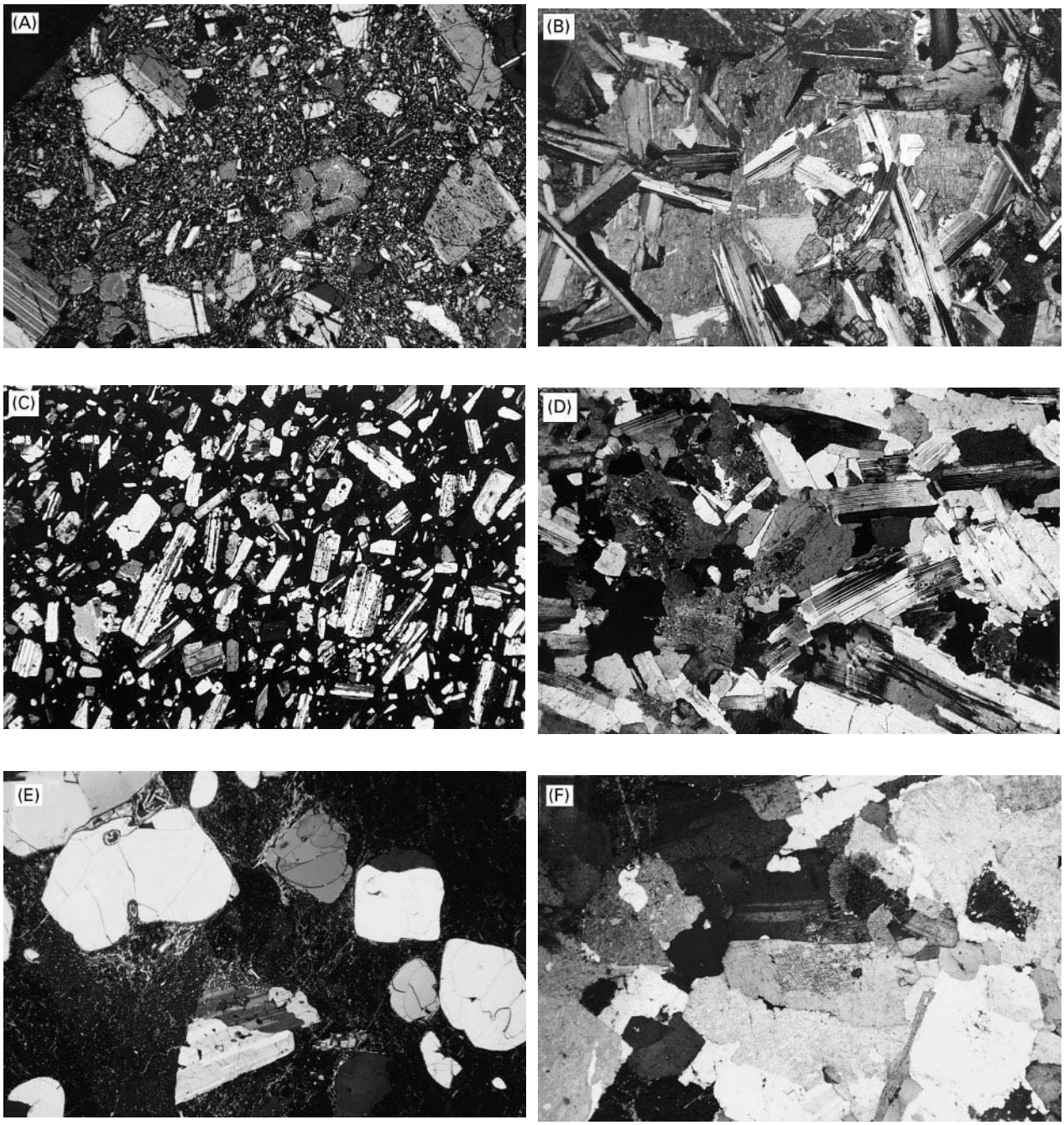

Figure 1 (See Colour Plate 33). Crossed polarizer photomicrographs of (a) a glassy basalt, (b) a gabbro, (c) an andesite, (d) a diorite, (e) a rhyolite and (f) a granite. Each of these photographs was taken at the same magnification (horizontal field is 10 mm across). The bulk composition of the magma forming the basalt and gabbro are broadly similar, as is the bulk composition for the andesite and diorite and the rhyolite and granite. The minerals crystallizing from the basalt and gabbro are similar, as are those in the andesite and diorite and the rhyolite and granite. The clearly observable differences in texture result from differences in crystal growth and nucleation rates. (a) Basalt showing large crystals (phenocrysts) of plagioclase feldspar (grey), Ca-rich pyroxene (purple, at centre) and olivine (yellow, top left) in a finer grained groundmass of these minerals. (b) Gabbro showing crystals of Ca-rich pyroxene (red-orange) enclosing plagioclase (grey-white with multiple twinning) and olivine (blue, green and red grains right of centre). (c) Andesite showing phenocrysts of plagioclase (grey-white with multiple twinning) and pyroxene (yellow, orange-red) set in a fine grained glassy groundmass. (d) Diorite showing a rock comprised of plagioclase feldspar (grey-white multiply twinned crystals), pyroxene, amphibole (green) and interstitial quartz (yellow-grey). Note how the amphibole crystals form a jacket or coating on the pyroxene (centre). (e) Rhyolite showing perlitic cracking in glassy groundmass and phenocrysts of quartz and plagioclase (twinned). Note the corroded and resorbed grain boundaries of the phenocrysts. (f) Granite showing interlocking crystals of plagioclase (twinned), alkali feldspar (turbid, dusty appearance), quartz (clear) and biotite (speckly orange).

the fact that they are less dense and less viscous than their surroundings. Ultimately, they may be emplaced at shallower levels in the Earth, forming igneous intrusions such as batholiths, plutons and sills or erupted at the surface as lava flows or pyroclastic rocks.

Because they are multicomponent melt systems, on cooling, magmas will crystallize a variety of silicate minerals, whose composition is controlled by the bulk composition of the magma and whose grain size is determined by the rates of cooling and crystal nucleation (**Figure 1**). Thus basaltic magmas will crystallize Ca-rich pyroxene, Ca-rich plagioclase, Fe-Ti oxides and perhaps olivine, whereas granitic magma will crystallize Na-rich plagioclase, K-rich alkali fieldspar, quartz and mica. The ultimate example of undercooling is a natural glass, called obsidian in the case of rhyolite and tachylite in the case of basalt. In nature, volcanic rocks are frequently a mixture of crystals (which grew at depth in the earth) and glass (which quenched on eruption). Intrusive rocks are more likely to be crystalline, with the interlocking minerals displaying a variety of textures

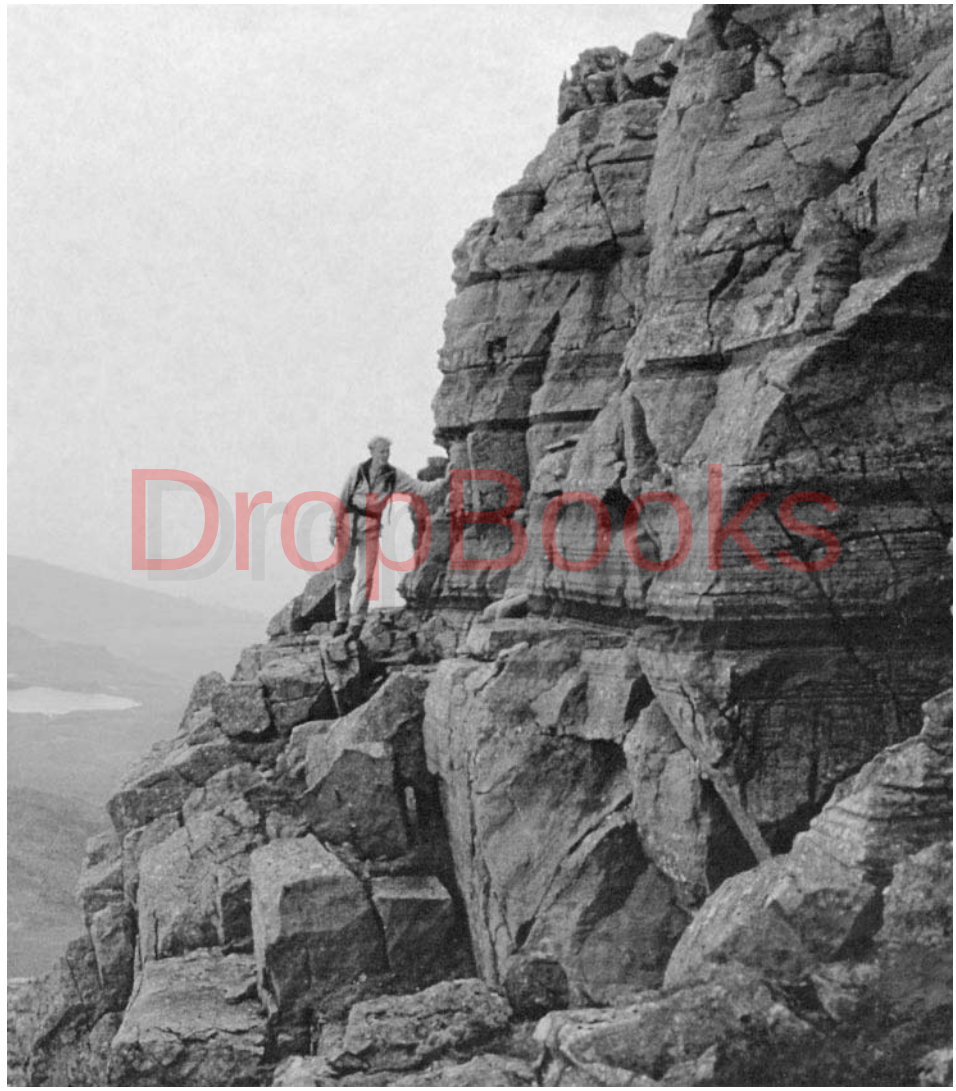
DropBooks

Figure 2 (See Colour Plate 35). Mineral layering in the Rum Igneous Intrusion, NW Scotland. This photograph shows spectacular centimeter-scale mineral layering in Unit 14 of the Eastern Layered Series of the Rum Layered Igneous Intrusion. The Rum Intrusion forms one of a number of layered intrusions, including Skaergaard in East Greenland and The Cullins, on Skye, NW Scotland, which are part of the North Atlantic Tertiary Igneous Province. Now exhumed by the combined effects of erosion and uplift, these intrusions mark the site of crystallizing magma chambers $\sim$ 60 million years ago, during the early rifting stages of the North Atlantic Ocean. The near horizontal layers were formed by sequential precipitation of crystals of different composition (principally plagioclase, pyroxene, olivine and spinel) on the floor of a magma chamber. The darker layers are rich in the minerals olivine and pyroxene, the lighter layers richer in plagioclase. Mimicking sedimentary rocks where the principal hydraulic agent of sorting is a water column, in layered intrusions magma was the hydraulic agent and dense minerals, like spinel and olivine, settled more rapidly than plagioclase, leading to units which are graded from spinel and olivine-rich bases to plagioclase-rich tops.

reflecting the crystallization history of the magma (Figure 1). The minerals crystallizing from the basalt magma are higher temperature solid solutions than those of the granite magmas, deriving from their bulk composition and the higher temperatures of basaltic magmas.

The pioneering high-temperature experimental studies on the effects of magmatic crystallization was undertaken by N.L. Bowen and coworkers during the first half of twentieth century and laid the foundations for understanding how magmas evolve by crystallization. Bowen's textbook, *The Evolution of the Igneous Rocks*, first publised in 1928, remains the definitive exposition on the application of phase equilibria to the study of magmatic crystallization. In this book, Bowen championed the role of fractional crystallization as the process most responsible for producing diversity in magmatic rocks. This work received a considerable boost by the discovery of the Skaergaard Intrusion in East Greenland by L.R. Wager in 1931 and subsequent mapping of the intrusion by Wager and W.A. Deer. Here, graphic demonstration of the effects of crystal settling layering and the results of fractional crystallization were to spawn an array of terminology and another benchmark text, *Layered Igneous Rocks*. Layered igneous intrusions (**Figure 2**) are now known to be important examples of subvolcanic magmatic systems where the processes of magmatic differentiation have been preserved.

Phase diagrams remain the most elegant way of appreciating how magmatic crystallization proceeds. **Figure 3** is the phase system diopside ($MgCaSi_2O_6$)–anorthite ($CaAl_2Si_2O_8$)–albite ($NaAlSi_3O_8$) at 1 atm. This system makes a simple proxy for a basaltic magma because it consists of the two major minerals in basalt, plagioclase feldspar (anorthite–albite solid solution) and Ca-rich pyroxene (diopside). The diagram is divided into two primary stability fields by the curved, arrowed line from 1275°C at *e* to ~1100°C at *e*′. The upper field is that of diopside, the lower field that of plagioclase (solid solution). The curved line delineates a cotectic of falling temperature

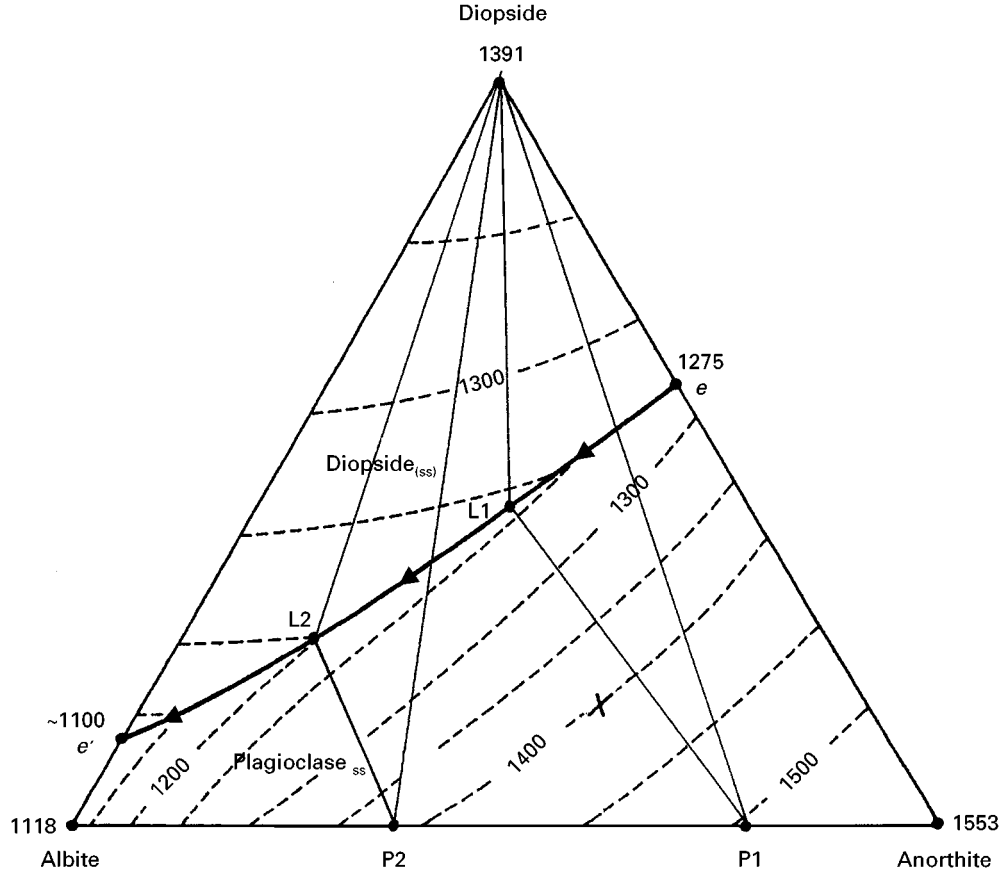

Figure 3 The phase system diopside–anorthite–albite at 1 atm. This system is a particularly useful analogue for the basaltic magma system as it comprises the two major minerals which crystallize from basalt magma, Ca-rich pyroxene (diopside, $MgCaSi_2O_6$) and plagioclase feldspar (solid solution, ss, between anorthite ($CaAl_2Si_2O_8$) and albite ($NaAlSi_3O_8$)). In this system cooling melts will evolve along the diopside–plagioclase cotectic from right (high temperature) to left (low temperature). Note that in a cooling, crystallizing magmatic system, a liquid (L1) will be in equilibrium with crystals of diopside and plagioclase of composition P1. With cooling, L1 will migrate to L2 and here L2 will be in equilibrium with crystals of diopside and lower temperature plagioclase, P2.

(in direction of arrows) and along which changing liquid compositions will be in equilibrium with diopside and progressively different (lower temperature) compositions of plagioclase. Liquids (L1 and L2) lying along the curve (e–e') will be in equilibrium with diopside and two plagioclase compositions (P1 and P2) such that the lower temperature liquid L2 is in equilibrium with a lower temperature, more sodic, plagioclase (P2).

The process of magmatic fractional crystallization can also be demonstrated effectively through the use of geochemistry. For example, in **Figure 4**, two bivariate plots of SiO_2 and CaO versus MgO (all in weight percent) are shown for a hypothetical parent magma which is cooling and fractionating olivine $[(Mg_2SiO_4)_{90}.(Fe_2SiO_4)_{10}]$. Note that removal and addition of olivine to the 'parent' magma results in changes to the compositions of the resultant melts. Addition of olivine produces MgO enrichment, removal (extraction) of olivine produces MgO-depleted melts. A further application of this approach is illustrated in **Figure 5**, which uses the total alkali ($Na_2O + K_2O$) versus SiO_2 diagram, often referred to as the TAS diagram, and the internationally recommended means for classifying volcanic igneous rocks. Data points for a suite of analysed volcanic rocks have been added to this diagram and depict a trend of increasing total alkalis with increasing SiO_2. Between 55 and 56% SiO_2 the trend splits, with one set of data showing relative enrichment in alkalis. These trends are readily explained by changes in the bulk composition of the fractionating mineral assemblages.

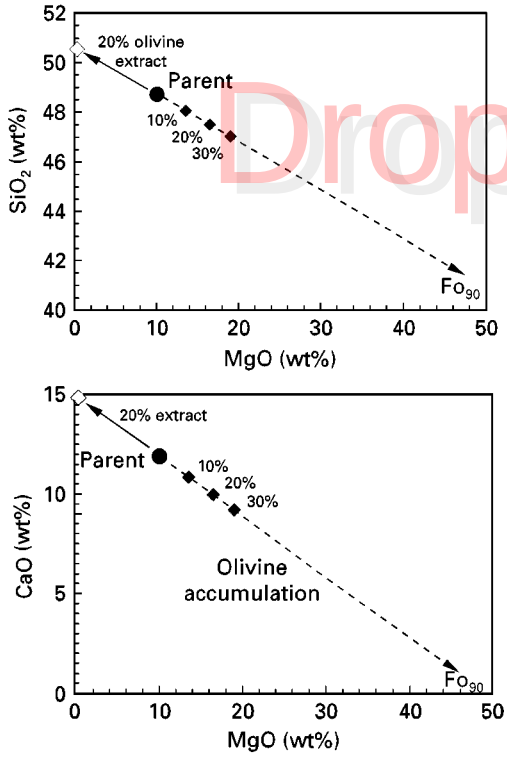

Figure 4 Chemical variation diagrams showing effects of olivine removal and addition to a hypothetical basalt parent magma. Olivine is a relatively simple orthorhombic silicate mineral and crystallizes as a solid solution of Mg_2SiO_4 (forsterite, Fo) and Fe_2SiO_4 (fayalite, Fa) end-members. In basaltic magmas, crystallizing olivine is typically Mg-rich, usually around Fo_{90}, consistent with the high temperatures of these magmas. Removal of Mg-rich olivine will rapidly deplete the residual liquid in MgO. Conversely, addition or accumulation of olivine in the melt will increase MgO.

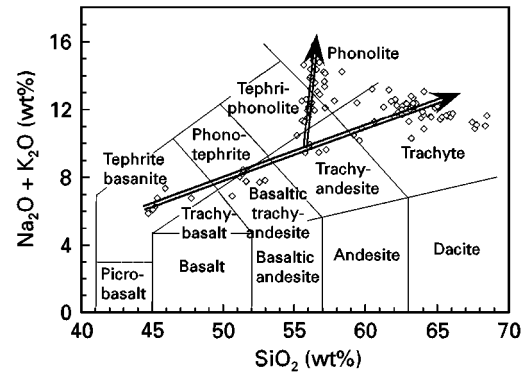

Figure 5 Total alkalis ($Na_2O + K_2O$, wt%) versus SiO_2 (wt%) for a suite of chemically analysed volcanic rocks (◇) which have evolved from a parent (tephrite basanite) composition by fractional crystallization. The bifurcation in the trend derives from a change in the mineral proportions in the fractionating mineral assemblage, around 55–56% SiO_2, one leading to phonolite the other leading to trachyte.

The importance of the process of crystallization in the evolution of magmas and igneous rocks is clear. Through fractional crystallization, which is the natural consequence of a cooling, crystallizing multicomponent magmatic system, a wide spectrum of compositions of igneous rocks can be produced. This, together with the depth at which partial melting takes place, is the major process responsible for producing diversity amongst terrestrial igneous rocks.

See Colour Plates 33, 34, 35.

Further Reading

Bowen NL (1928) *The Evolution of the Igneous Rocks*. New York: Princeton University Press.

Cox KG, Bell JD and Pankhurst RJ (1979) *The Interpretation of Igneous Rocks*. London: George Allen and Unwin.

Ehlers EG (1972) *The Interpretation of Geological Phase Diagrams*. San Francisco: WH Freeman.

Le Maitre RW, Bateman P, Dudek A, Keller J *et al.* (eds) (1989) *A Classification of Igneous Rocks and Glossary of Terms*: *Recommendations of the International Union of Geological Sciences Subcommission on the Systematics of Igneous Rocks*. Oxford: Blackwell Scientific Publications.

McBirney AR (1993) *Igneous Petrology* (2nd edn). Boston and London: Jones and Bartlett Publishers.

Wager LR and Brown MG (1968) *Layered Igneous Rocks*. Edinburgh: Oliver and Boyd.

DropBooks